


Enhanced TEMPO Algorithm for Quantum Path Integrals with Off-Diagonal System-Bath Coupling: Applications to Photonic Quantum Networks

Marten Richter^{1,*} and Stephen Hughes²

¹*Institut für Theoretische Physik, Nichtlineare Optik und Quantenelektronik, Technische Universität Berlin, Hardenbergstr. 36, EW 7-1, 10623 Berlin, Germany*

²*Department of Physics, Engineering Physics, and Astronomy, Queen's University, Kingston, Ontario K7L 3N6, Canada*

 (Received 5 October 2021; accepted 23 March 2022; published 22 April 2022)

Multitime system correlation functions are relevant in various areas of physics and science, dealing with system-bath interaction including spectroscopy and quantum optics, where many of these schemes include an off-diagonal system bath interaction. Here we extend the enhanced time-evolving matrix product operator (eTEMPO) algorithm for quantum path integrals using tensor networks [Phys. Rev. Lett. **123**, 240602 (2019)] to open quantum systems with off-diagonal coupling beyond a single two level system. We exemplify the approach on a coupled cavity waveguide system with spatially separated quantum two-state emitters, though many other applications in material science are possible, including entangled photon propagation, photosynthesis spectroscopy, and on-chip quantum optics with realistic dissipation.

DOI: 10.1103/PhysRevLett.128.167403

The theory of open quantum systems remains a very active focus of current research [1–13], since it provides answers to many questions related to quantum computing, entanglement and communication, and also quantum networks. The theoretical frameworks include tensor network (TN) methods [12,14–24] and quantum path integrals [2,3,6–8,10–13]. Recently these two approaches were successfully combined [11–13,25], exploiting their combined advantages in the TEMPO (time-evolving matrix product operator) algorithm [11,26] and an enhanced TEMPO (eTEMPO) algorithm [25]. Applications so far have mainly studied a two level system (TLS) *diagonally* coupled to an external bath [10–13,25–27]. Beside these examples, many important problems remain to be studied in more detail, ranging from exciton relaxation in photosynthetic light harvesting systems [28–31] or nanostructures to exploit photon propagation, entanglement, superradiance, and feedback [12,22,32–40]—which require *off-diagonal* system bath coupling. Mostly their treatment requires other algorithms, such as hierarchical equations of motion [31,41,42], and alternative TNs [12,22,42,43].

Here we extend the eTEMPO method to include off-diagonal coupling as opposed to extending the TEMPO algorithm [44]. As input, we require only the generalized bath correlation function; in contrast to Ref. [45], where bath degrees of freedom are included and accessible in the network propagation, we show the effect of retardation for a two-cavity waveguide system on the first two rungs of photon transition. We demonstrate how the system transitions between one single generalized Jaynes-Cummings model (JCM) to a retardation regime between two JCMs,

including a subradiant state. This manifests in a highly nontrivial non-Markovian dynamic, whose features *cannot* be captured with linearized response functions nor phenomenological JCMs.

Theoretically, a typical open quantum system has system H_s and bath H_b Hamiltonian. Figure 1 shows an example of an integrated waveguide system, which is representative of emerging experiments with integrated semiconductor quantum dot systems [46–56]. The bath is harmonic, so Wick's theorem holds for factorizing initial conditions [57]. We consider a linear system-bath interaction $H_{sb} = \sum_{ij\mu} C_{ij\mu} A_{ij} B_{\mu}$, where $C_{ij\mu}$ are the system-bath coupling constants, $A_{ij} = |i\rangle_s \langle j|_s$ (here in particular including $i \neq j$), and B_{μ} is a linear bath operator; for a harmonic bath, $\text{tr}(B_{\mu} \rho_B) = 0$. The dynamics of the full system-bath density matrix operator ρ obeys $\partial_t \rho = -(i/\hbar)(H_{s,-} + H_{b,-} + H_{sb,-})\rho$, where the subscripts $-$, $+$, L , R convert a

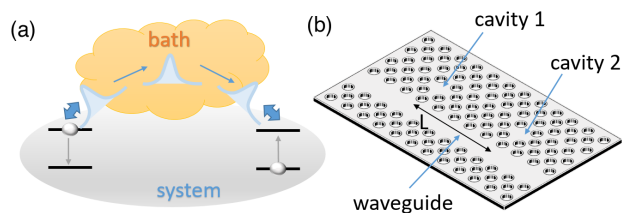


FIG. 1. (a) Open quantum system coupled to a bath with excitation transfer through the bath. (b) Example system: photonic crystal with waveguide and two cavities separated by length L with a quantum emitter (TLS) in each cavity.

Hilbert space operator D to a Liouville space operator [28] with $D_L \rho = D \rho$ and $D_R \rho = \rho D$, and also $D_- = D_L - D_R$. Notably, the method can also include Lindblad operators for system dynamics together with $H_{s,-}$. The time dynamics can be solved via the time ordered exponential $U(t, t_0) = T_{\leftarrow} \exp(-i/\hbar \int_{t_0}^t H_-(\tau) d\tau)$ in Liouville space, $\rho(t) = U(t, t_0) \rho(t_0)$. Our observables of interest are multi-time correlation functions $\langle T_{\leftarrow} A_1(t_1) \cdots A_N(t_N) \rangle$ with Liouville operators A_1, \dots, A_N .

Next, we convert the correlation function into a quantum path integral formulation [2,3,6–8,10–13]; this allows us to develop an extended algorithm for systems with off-diagonal system-bath coupling, based on the eTEMPO algorithm [25]—which is a very efficient algorithm for many quantum path integral TN implementations [11–13]. To proceed, we divide time t into intervals ΔT such that $t_n = n \Delta T$ with integer n . The times in the multitime correlation function should obey $t_i = \Delta T n_i$ with integer n_i , and we obtain $\langle T_{\leftarrow} A_1(t_1) \cdots A_N(t_N) \rangle = \text{tr}[O_M U_{M-1} \cdots U_1 O_1 U_0 O_0 \rho(t_0)]$, with $O_n = A_k$ if $t_k = \Delta T n$ for any k ; otherwise $O_n = Id$. U_i is defined as $U_i = U(t_{i+1}, t_i)$. For most path integral implementations, the Suzuki-Trotter formula is applied to separate system and bath for the influence functional. We use perturbation theory and the Feynman disentangle theorem. Perturbation theory to a limited order fails for processes involving many interactions over all times; thus, we apply perturbation theory to the individual intervals ΔT , so to each U_i , keeping often only one system-bath process per ΔT . For sufficient small ΔT , compared to system-bath coupling, a nonperturbative result is obtained with numerical accuracy. In general, $U_i = U_0(t_{i+1}, t_{i+\frac{1}{2}}) U_i^{(i)} U_0(t_{i+\frac{1}{2}}, t_i)$, with $U_i^{(i)} = T_{\leftarrow} \exp(-i/\hbar \int_{t_i}^{t_{i+\frac{1}{2}}} U_0(t_{i+\frac{1}{2}}, \tau) H_{sb,-} U_0(\tau, t_{i+\frac{1}{2}}) d\tau)$.

Restricting the system-bath coupling $H_{sb,-}$ to first order, per ΔT [and second-order for nonvanishing bath correlation function, as explained after Eq. (3)], yields

$$\begin{aligned}
 U_i &= U_0(t_{i+1}, t_{i+\frac{1}{2}}) U_{sb,i} U_0(t_{i+\frac{1}{2}}, t_i) \\
 U_{sb,i} &= \left(Id - \frac{i}{\hbar} \int_{t_i}^{t_{i+1}} d\tau U_0(t_{i+\frac{1}{2}}, \tau) H_{sb,-} U_0(\tau, t_{i+\frac{1}{2}}) \right. \\
 &\quad \left. - \frac{1}{\hbar^2} \int_{t_i}^{t_{i+1}} d\tau_1 \int_{t_i}^{\tau_1} d\tau_2 U_0(t_{i+\frac{1}{2}}, \tau_1) \right. \\
 &\quad \left. H_{sb,-} U_0(\tau_1, \tau_2) H_{sb,-} U_0(\tau_2, t_{i+\frac{1}{2}}) \right), \quad (1)
 \end{aligned}$$

with the time evolution operator $U_0(\cdot, \cdot)$ containing solely $H_{s,-}$ and $H_{b,-}$. The symmetric expansion with $U_0(\cdot, \cdot)$ on the left and right allows one to exclude (include) certain parts of the Hamiltonian (e.g., like external optical excitation) in the inner brackets. Including second-order contributions from the same ΔT (cf. cumulant expansions [58]) prevents an

artificial minimum delay between system-bath interactions and reducing ΔT dependency, and thus recovers simple perturbation theory for weak coupling. We define $U_{0,i+\frac{1}{2}}^{\frac{1}{2}} = U_0(t_{i+\frac{1}{2}}, t_i)$ and rewrite $U_{sb,i} = U_{sb,i}^{(0)} + U_{sb,i}^{(1)} + U_{sb,i}^{(2)}$, with the k th order system-bath contribution $U_{sb,i}^{(k)}$; $H_{sb,-}$ contains system A and bath operators B , so we apply $(AB)_- = A_+ B_- + A_- B_+$. Finally, $U_{sb,i}^{(k)}$ can be written as $U_{sb,i}^{(k)} = \sum_l A_l^{(k)} B_l^{(k)}$ with Liouville system operators $A_l^{(k)}$ and bath operators $B_l^{(k)}$ (each with a maximum k linear bath operators).

With an initial factorizing density matrix $\rho(t_0) = \rho_s \otimes \rho_b$, then

$$\begin{aligned}
 &\langle T_{\leftarrow} A_1(t_1) \cdots A_N(t_N) \rangle \\
 &= \sum_{k_{M-1}, \dots, k_0=0}^2 \sum_{l_{M-1}, \dots, l_0} \text{tr}_b(U_{b, M-\frac{1}{2}} B_{l_{M-1}}^{(k_{M-1})} \cdots U_{b, \frac{1}{2}} B_{l_0}^{(k_0)} \rho_b) \\
 &\quad \cdot \text{tr}_s(O_M U_{s, M-\frac{1}{2}} A_{l_{M-1}}^{(k_{M-1})} \cdots O_1 U_{s, \frac{1}{2}} A_{l_0}^{(k_0)} U_{s,0}^{\frac{1}{2}} O_0 \rho_s), \quad (2)
 \end{aligned}$$

holds with the bath $U_{b,i}$ and system $U_{s,i}$ time propagation. For initial thermal correlated $\rho(t_0)$, a Liouville operator A_c can be included in O_0 [59], while keeping a harmonic ρ_b in Eq. (2).

To convert the expressions to a quantum path integral, we insert Liouville space identities: $Id = \sum_{s_L, s_R} (|s_L\rangle\langle s_L|)_L (|s_R\rangle\langle s_R|)_R$, using an H_s eigenbasis. Using the notation $A = \sum_{s,p} A_{p_R s_L}^{p_L s_L} (|p_L\rangle\langle s_L|)_L (|s_R\rangle\langle p_R|)_R$ for expanding any operator A , we obtain $\langle T_{\leftarrow} A_1(t_1) \cdots A_N(t_N) \rangle = \sum_{\{k\}\{s\}\{p\}} I(s_0, p_1, s_1, \dots, p_M, s_M) \text{tr}_s[\tilde{O}_{s_M p_M} \cdots \tilde{O}_{s_1 p_1} \tilde{\rho}_{s_0 p_0}]$, with the convention $\{x\} = x_1, \dots, x_M$ for indices and with $\tilde{O}_{s_n p_n} = (O_n U_{s, n-1/2})_{s_n p_n}$ and $\tilde{\rho}_{s_0 p_0} = (U_{s,0}^{\frac{1}{2}} O_0 \rho_s)_{s_0 p_0}$. Without subscripts L or R , an index includes left and right Liouville space. We replace the index l and the operators $A_l^{(k)}$ with indices s and p , and an according redefinition of operator matrix elements $B_{k_j}^{(p_j s_j)}$ including the free bath propagation (and indicating the interval with index j) in the influence functional I , so that $I(s_0, p_1, k_1, \dots, p_M, s_M, k_M) = \text{tr}_B(B_{k_{M-1}}^{(p_M s_{M-1})} \cdots B_{k_1}^{(p_2 s_1)} B_{k_0}^{(p_1 s_0)} \rho_b)$.

Wick's theorem holds for factorization, since the harmonic bath is initially in thermal equilibrium (no photons). Thus, I factorizes into expectation values of two linear bath operators, with each linear bath operator from a different interval ΔT or two from the same interval ΔT . We arrive at an iterative expression for I :

$$\begin{aligned}
 I(s_0, p_1, k_1) &= E_{s_0 p_1 k_1}, \\
 I(s_0, p_1, k_1, \dots, s_M, p_{M+1}, k_{M+1}) &= E_{s_M, p_{M+1}, k_{M+1}} I(s_0, p_1, k_1, \dots, s_{M-1}, p_M, k_M) \\
 &\quad + \delta_{k_{M+1}, 1} \sum_{m=1}^M \delta_{k_m, 1} M_{s_M, p_{M+1}, k_{M+1}}^{p_{m+1} s_m} I(s_0, p_1, k_1, \dots, s_{m-1}, p_m, -1, \dots, s_{M-1}, p_M, k_M), \quad (3)
 \end{aligned}$$

where $E_{s,p,k}$ describes the current time interval with zero (δ_{sp}), two ($B_2^{(ps)}$) or one system-bath interactions, and $k = -1$ is added to link to previous times: $E_{s,p,k} = [\delta_{sp} \delta_{k,0} + \delta_{k,2} \text{tr}_b(B_2^{(ps)} \rho_B) + \delta_{k,-1}]$. Here $M_{s_M, p_{M+1}, k_{M+1}}^{p_{m+1} s_m}$ describes a process, with one interaction in the interval m (e.g., photon emission) and one in the interval $M+1$ (e.g., photon absorption): $M_{s_M, p_{M+1}, k_{M+1}}^{p_{m+1} s_m} = \delta_{k_{M+1}, 1} \text{tr}_b(B_1^{(s_M, p_{M+1})} B_1^{(s_m, p_{m+1})} \rho_b)$, and depends only on the time difference $M - m$ for time independent bath Hamiltonians.

Note that $M_{s_M, p_{M+1}, k_{M+1}}^{p_{m+1} s_m}$ contains a generalized bath correlation function, directly connected to a generalized

spectral density for off-diagonal coupling [28], which fully determines the system-bath interaction. The tensor M describes a boson going into the bath at m and back to the system at $M+1$. We discuss differences to the quantum path integrals with diagonal coupling—the standard influence functional [2,3,6–8,10–13,25]. For the common case, the I depends only on one index s per ΔT , where for the off-diagonal case it depends on initial s and final p index and the k the number of system-bath interactions per ΔT . We note, hitherto, most numerically exact treatments with TN focused only on diagonal coupling.

We reformulate Eq. (3) for easier conversion to a TN:

$$\begin{aligned}
 I(s_0, p_1, k_1, \dots, s_M, p_{M+1}, k_{M+1}) \\
 = \sum_{\{k'\} \{l\} \{\alpha_p\} \{\alpha_s\}} \prod_{m=1}^M \tilde{E}_{s_M p_{M+1} k_{M+1}}^{\alpha_p \alpha_s l} \tilde{M}_{p_{m+1} s_m k_m \alpha_p \alpha_s l_m}^{k'_m \alpha_{p_{m-1}} \alpha_{s_{m-1}} l_{m-1}}(n) I(s_0, p_1, k'_1, \dots, s_{M-1}, p_M, k'_M) \delta_{\alpha_{p_1}, 1} \delta_{\alpha_{s_0}, 1} \delta_{l_1, 1}, \quad (4)
 \end{aligned}$$

with modified tensors \tilde{M} and $n = M + 1 - m$:

$$\tilde{M}_{psk\alpha_p \alpha_s l}^{k' \alpha'_p \alpha'_s l'}(n) = \delta_{k,1} \delta_{k',-1} \delta_{\alpha'_p, 1} \delta_{\alpha'_s, 1} \delta_{l,1} G_{psl\alpha_p - 1 \alpha_s - 1}(n) + \delta_{k,k'} \delta_{\alpha_p, \alpha'_p} \delta_{\alpha_s, \alpha'_s} \delta_{l,l'}, \quad (5)$$

where $G(n)$ is the double integrated system-bath correlation function [Eq. (1)] between two ΔT intervals, which are $n\Delta T$ apart. The first interaction acts on the left (right) side in Liouville space for $l = 1$ ($l = 2$) respectively, changing the left or right state from $\alpha_s - 1$ to $\alpha_p - 1$. $\alpha'_{p/s} = 1$ encodes no further interaction in subsequent ΔT . In Eq. (5) the modified tensor \tilde{E} appears as

$$\tilde{E}_{s,p,k}^{\alpha_p, \alpha_s l} = [\delta_{k,0} \delta_{sp} + \delta_{k,2} G_{ps} + \delta_{k,-1} + \delta_{k,1} (\delta_{l,1} \delta_{\alpha_p, p_L+1} \delta_{\alpha_s, s_L+1} + \delta_{l,2} \delta_{\alpha_p, p_R+1} \delta_{\alpha_s, s_R+1})], \quad (6)$$

where the C tensor contains the system-bath correlation within the first interval ΔT .

Equation (4) is now converted to a TN, where we depict a tensor, e.g., T_{ijk} , as a rectangle and each index i , j , and k as a line [cf. Fig. 2(a)], where connected indices between tensors indicate a summation [15]. The TN depicted in Fig. 2(b), built up from tensors \tilde{E} and \tilde{M} , can be contracted by interpreting the first row as a matrix product state (MPS) and the subsequent rows as a matrix product operator (MPO), and applying MPOs to the MPS subsequently [15]. The TN is the TEMPO [11] implementation for the off-diagonal case.

Because of the increased tensor rank in the off-diagonal case, the TEMPO algorithm is highly ineffective especially beyond a single TLS. Here we construct a TN that reduces the index dimension and yields the original tensors after contraction. Therefore, we design a product of 6 (and 7) low rank and low dimensional tensors that yield $\tilde{M}^{(c)}$ (and \tilde{E}). These are also decomposed into a MPS [60] and the resulting MPSs are connected via δ tensors to obtain the TN of MPOs in Fig. 2(c). Further details are given in the Supplemental Material [61].

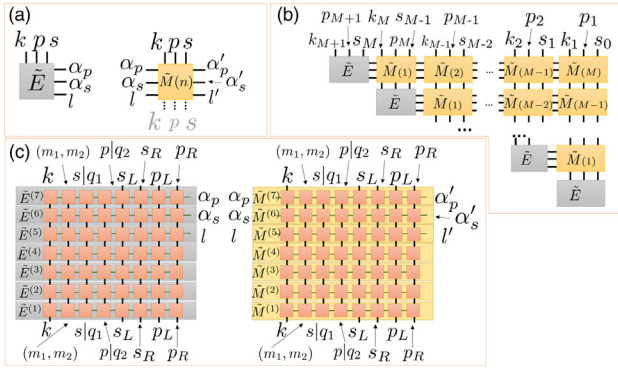


FIG. 2. (a) Tensors \tilde{E} and \tilde{M} depicted as rectangle and indices. (b) TN for the influence functional from Eq. (4). (c) Decomposition of the \tilde{E} and \tilde{M} into seven matrix product operators (indices are connected with delta tensors).

Following the idea from Ref. [25], that the indices on \tilde{E} can be moved to the other edge of the network from Fig. 2(b) (rotating the TN by ninety degrees), we obtain the decomposed TN as in Fig. 3. Then the TN (Fig. 3), including the temporal propagation of the system from Eq. (4), is contracted to obtain the expectation values. For evaluation, the MPOs are applied row by row [Figs. 4(a)–4(c), Eq. (3) using *exactly* apply from itensor [65]], thus implementing the eTEMPO algorithm [25] variant for the off-diagonal case in itensor (version 2.1.0 patched) [65]. Tensors in the MPS

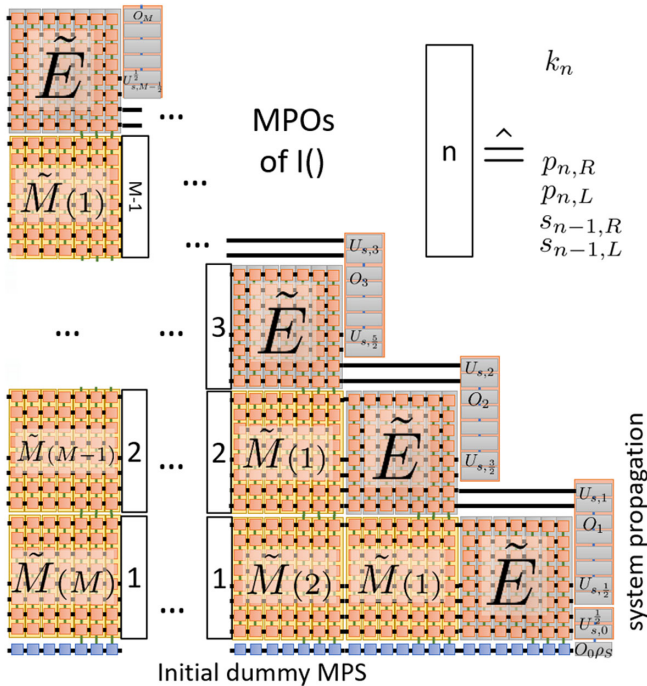


FIG. 3. TN for $\langle T_{\leftarrow A_1}(t_1) \dots A_N(t_N) \rangle$. On the right edge of the TN the MPS decomposed system propagators $U_{s,m-1/2}$ [cf. Eq. (2)] are connected to the indices s and p . The majority of the network is constructed from the decomposed \tilde{M} and \tilde{E} tensors. An initial MPS is at the bottom.

connected to previous times are traced out, achieving a massive reduction of computational time (cf. Fig. 4). Then a row of blocks in the network are added to the current MPS to extend the covered time, if required.

Critically, our framework is capable of including both diagonal and off-diagonal coupling and is thus applicable to a multitude of problems, including exciton-phonon dynamics in (coupled) nanostructures [8,66–70], photosynthetic pigment-protein complex [29,30,71], and quantum optics systems including plasmonics [12,32–36,72,73]. To demonstrate the power of our approach, we consider a *quantum network example*, with *on-chip photonic propagation*, fully consistent with a rigorous Maxwell solution theory of a photonic crystal with a waveguide and two integrated cavities [74] as depicted in Fig. 1(b) (system parameters in Ref. [61]). This scheme is also timely with recent experiments [75].

We assume a TLS with $H_s = \sum_l \epsilon_i |i\rangle_l \langle i|_l$, in each cavity, where ϵ_i is the energy of level i in system l . The photonic crystal medium can be quantized using the Green's function $\mathbf{G}(\mathbf{r}, \mathbf{r}', \omega)$ of the Helmholtz equation [61,74,76]. The electric field operator is $\mathbf{E}(\mathbf{r}, \omega) = i\sqrt{(\hbar/\pi\epsilon_0)} \int d^3r' \sqrt{\epsilon_l(\mathbf{r}', \omega)} \mathbf{G}(\mathbf{r}, \mathbf{r}', \omega) \cdot \mathbf{b}(\mathbf{r}', \omega)$, where $\mathbf{b}(\mathbf{r}, \omega)$ are boson operators that form the bath for the path integral approach: $H_B = \hbar \int d^3r \int_0^\infty d\omega \omega \mathbf{b}^\dagger(\mathbf{r}, \omega) \cdot \mathbf{b}(\mathbf{r}, \omega)$. A dipole coupling $\mathbf{d}_{ij}^{(i)}$ for the i emitter at position \mathbf{r}_i to the bath constitutes the system-bath interaction $H_{sb} = \sum_{nij} |i\rangle_n \langle j|_n \mathbf{d}_{ij}^{(n)} \cdot \int_0^\infty d\omega \mathbf{E}(\mathbf{r}_n, \omega) + \text{H.a.}$. The correlation function $C_{ijkl}^{nm}(\tau) = (1/\hbar\pi\epsilon_0) \int d\omega e^{-i\omega\tau} \mathbf{d}_{ij}^{(n)} \cdot \text{Im}[G(\mathbf{r}_n, \mathbf{r}_m, \omega)] \cdot \mathbf{d}_{kl}^{*(m)}$ characterizes the system-bath coupling and dynamics and therefore is also present in the decomposed tensors G [61] via $G_{ijkl}^{nm(\tilde{i})} = -\int_{t_i}^{t_{i+1}} d\tau_1 \int_{t_i}^{\tau} d\tau_2 e^{i(\epsilon_i - \epsilon_j)\tau_2 + i(\epsilon_k - \epsilon_l)\tau_1} \times C_{ijkl}^{nm}(\tau_2 - \tau_1)$ and $G_{ijkl}^{nm(\tilde{j})} = -\int_{t_i}^{t_{i+1}} d\tau_1 \int_{t_j}^{t_{j+1}} d\tau_2 e^{i(\epsilon_i - \epsilon_j)\tau_2 + i(\epsilon_k - \epsilon_l)\tau_1} C_{ijkl}^{nm}(\tau_2 - \tau_1)$.

For our example system shown in Fig. 1(b), the TLSs are chosen resonant with the cavity modes. We excite the TLSs by a few-fs pulse described by

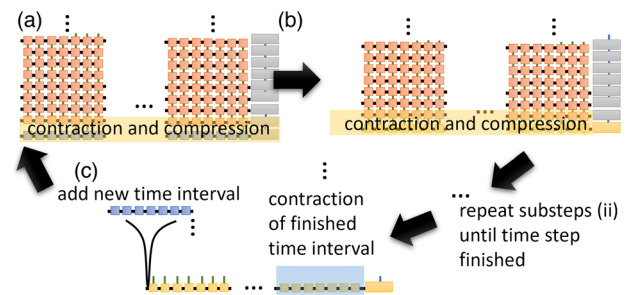


FIG. 4. (a) Application of next MPO to the current MPS (initially a dummy MPS) (b) repeated until all tensors of ΔT are contracted, then (c) removal of the current interval, and extension for future intervals. (a) Repeated, until finished.

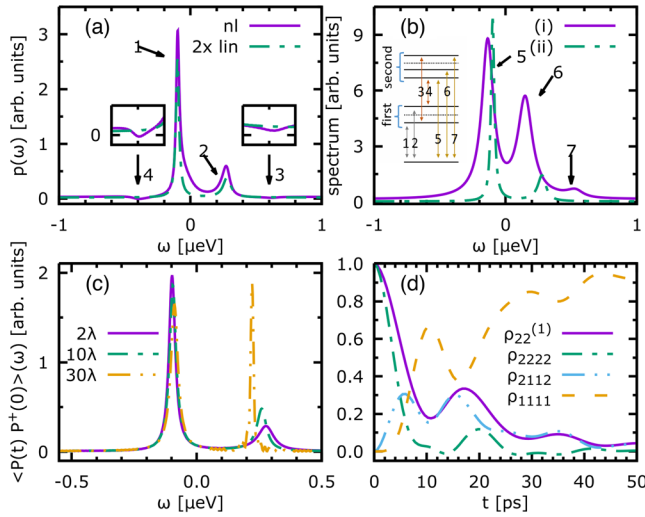


FIG. 5. (a) Nonlinear (nl) and linear (lin) spectra for the setup from Fig. 1(b) with a TLS resonant to both cavity frequencies. (b) Fourier transform of (i) double $\langle P(t)P(t)P^\dagger(0)P^\dagger(0) \rangle$ and (ii) single quantum $\langle P(t)P^\dagger(0) \rangle$ emitter polarization correlation function with $P^\dagger = \sum_l \mathbf{d}_l |2\rangle_l \langle 1|_l$ (inset JCM ladder). (c) Single quantum from (b) for different L . (d) Time dynamics of the upper level of reduced density matrix $\rho_{22}^{(1)}$ of one emitter, and for both emitters ρ_{mmmm} when both are initially excited.

$H_{\text{ext}} = \sum_l \mathbf{d} \cdot \mathbf{E}(t) e^{i\omega_l t} |2\rangle_l \langle 1|_l + \text{H.a.}$. The pulse does not excite the photons directly. A Fourier transform of the TLS polarization is shown in Fig. 5(a). Reference [77] the low intensity plot (linear spectrum) shows modified Rabi splitting between peaks 1 and 2 (cf. Ref. [74]) and the upper state [Eq. (2)] shows a lifetime broadening due to a transfer process to a lower state (e.g., state 1). A longer delay (increasing L , with the same phase) between the TLS affects the upper state, caused by an *intercavity* transfer of photons. So the long intercavity delay turns the upper state to a subradiant state with reduced broadening. Thus, the two cavities do not act as a single effective JCM model anymore; this is also true for the upper state in the higher rungs of the JCM ladder, which we study below.

For nonlinear excitation, shown also in Fig. 5(a) (0.45π , half excited), we observe additional (negative) peaks 3 and 4. A comparison to the energies in the single and double quantum function, in Fig. 5(b), indicates that these match well with transitions between the first and second rung of the JCM ladder. The single and double quantum function give the coherences of a system between ground state and single or double excitation states (respectively) [78–81] and allows for a direct inspection of their energies (see the Supplemental Material [61] for more details on our quantum correlation functions). Other (positive) contributions between the first and second rung are overlapping with resonances 1 and 2, which slightly affect their line shape. The negative peaks 3 and 4 appear only in our nonlinear solution, showing complex interference effects beyond weak excitation.

Although the origin of such line shapes are hard to identify, they may be related to an excitation transfer process [61]. The time dynamics of densities in Fig. 5(d) shows the typical Rabi oscillations. Furthermore correlations between the two TLS densities [Fig. 5(d)] allow access to complex entanglement properties.

We highlight that for many example systems, the bath correlation time is longer than the simulation time—a notoriously difficult test for the numerical complexity without augmenting the density matrix [8], yielding simulation times of days or weeks depending on the bath correlation time and excitation. Overall the example demonstrates the potential for eTEMPO algorithms where off-diagonal coupling is important to include.

In summary, we have provided a generalized version of the eTEMPO algorithm [25] to include off-diagonal system-bath coupling, opening the route for numerically exact treatment of off-diagonal system-bath coupling in exciton migration (e.g., coupled nanostructures, photosynthesis) or quantum light propagation in plasmonics and photonic networks. In particular, we have shown how delay and round trip coherence alter the JCM-like behavior.

We acknowledge funding from Queen’s University, the Canadian Foundation for Innovation, the Natural Sciences and Engineering Research Council of Canada, and support from the Alexander von Humboldt Foundation through a Humboldt Research Award.

*marten.richter@tu-berlin.de

- [1] H.-P. Breuer, F. Petruccione *et al.*, *The Theory of Open Quantum Systems* (Oxford University Press on Demand, New York, 2002), 10.1093/acprof:oso/9780199213900.001.0001.
- [2] A. Caldeira and A. Leggett, Path integral approach to quantum brownian motion, *Physica (Amsterdam)* **121A**, 587 (1983).
- [3] Y. Tanimura and S. Mukamel, Real-time path-integral approach to quantum coherence and dephasing in non-adiabatic transitions and nonlinear optical response, *Phys. Rev. E* **47**, 118 (1993).
- [4] J. Prior, A. W. Chin, S. F. Huelga, and M. B. Plenio, Efficient Simulation of Strong System-Environment Interactions, *Phys. Rev. Lett.* **105**, 050404 (2010).
- [5] M. Richter and A. Knorr, A time convolution less density matrix approach to the nonlinear optical response of a coupled system-bath complex, *Ann. Phys. (Amsterdam)* **325**, 711 (2010).
- [6] N. Makri and D. E. Makarov, Tensor propagator for iterative quantum time evolution of reduced density matrices. I. Theory, *J. Chem. Phys.* **102**, 4600 (1995).
- [7] N. Makri and D. E. Makarov, Tensor propagator for iterative quantum time evolution of reduced density matrices. II. Numerical methodology, *J. Chem. Phys.* **102**, 4611 (1995).
- [8] A. Vagov, M. D. Croitoru, M. Glässl, V. M. Axt, and T. Kuhn, Real-time path integrals for quantum dots: Quantum dissipative dynamics with superohmic environment coupling, *Phys. Rev. B* **83**, 094303 (2011).

- [9] A. W. Chin, A. Rivas, S. F. Huelga, and M. B. Plenio, Exact mapping between system-reservoir quantum models and semi-infinite discrete chains using orthogonal polynomials, *J. Math. Phys. (N.Y.)* **51**, 092109 (2010).
- [10] A. Strathearn, B. W. Lovett, and P. Kirton, Efficient real-time path integrals for non-Markovian spin-boson models, *New J. Phys.* **19**, 093009 (2017).
- [11] A. Strathearn, P. Kirton, D. Kilda, J. Keeling, and B. W. Lovett, Efficient non-Markovian quantum dynamics using time-evolving matrix product operators, *Nat. Commun.* **9**, 3322 (2018).
- [12] O. Kaestle, R. Finsterhoelzl, A. Knorr, and A. Carmele, Continuous and time-discrete non-Markovian system-reservoir interactions: Dissipative coherent quantum feedback in Liouville space, *Phys. Rev. Research* **3**, 023168 (2021).
- [13] E. V. Denning, M. Bundgaard-Nielsen, and J. Mørk, Optical signatures of electron-phonon decoupling due to strong light-matter interactions, *Phys. Rev. B* **102**, 235303 (2020).
- [14] R. Orús, A practical introduction to tensor networks: Matrix product states and projected entangled pair states, *Ann. Phys. (Amsterdam)* **349**, 117 (2014).
- [15] U. Schollwöck, The density-matrix renormalization group in the age of matrix product states, *Ann. Phys. (Amsterdam)* **326**, 96 (2011).
- [16] J. Cirac, D. Pérez-García, N. Schuch, and F. Verstraete, Matrix product density operators: Renormalization fixed points and boundary theories, *Ann. Phys. (Amsterdam)* **378**, 100 (2017).
- [17] F. Verstraete and J. I. Cirac, Matrix product states represent ground states faithfully, *Phys. Rev. B* **73**, 094423 (2006).
- [18] G. Vidal, Classical Simulation of Infinite-Size Quantum Lattice Systems in One Spatial Dimension, *Phys. Rev. Lett.* **98**, 070201 (2007).
- [19] S. R. Clark, J. Prior, M. J. Hartmann, D. Jaksch, and M. B. Plenio, Exact matrix product solutions in the Heisenberg picture of an open quantum spin chain, *New J. Phys.* **12**, 025005 (2010).
- [20] A. H. Werner, D. Jaschke, P. Silvi, M. Kliesch, T. Calarco, J. Eisert, and S. Montangero, Positive Tensor Network Approach for Simulating Open Quantum Many-Body Systems, *Phys. Rev. Lett.* **116**, 237201 (2016).
- [21] R. Rosenbach, J. Cerrillo, S. F. Huelga, J. Cao, and M. B. Plenio, Efficient simulation of non-Markovian system-environment interaction, *New J. Phys.* **18**, 023035 (2016).
- [22] H. Pichler and P. Zoller, Photonic Circuits with Time Delays and Quantum Feedback, *Phys. Rev. Lett.* **116**, 093601 (2016).
- [23] F. A. Schröder, D. H. Turban, A. J. Musser, N. D. Hine, and A. W. Chin, Tensor network simulation of multi-environmental open quantum dynamics via machine learning and entanglement renormalisation, *Nat. Commun.* **10**, 1062 (2019).
- [24] A. D. Somoza, O. Marty, J. Lim, S. F. Huelga, and M. B. Plenio, Dissipation-Assisted Matrix Product Factorization, *Phys. Rev. Lett.* **123**, 100502 (2019).
- [25] M. R. Jørgensen and F. A. Pollock, Exploiting the Causal Tensor Network Structure of Quantum Processes to Efficiently Simulate non-Markovian Path Integrals, *Phys. Rev. Lett.* **123**, 240602 (2019).
- [26] A. Strathearn, *Modelling Non-Markovian Quantum Systems Using Tensor Networks* (Springer Nature, Berlin, 2020), 10.1007/978-3-030-54975-6.
- [27] J. Kabuss, A. Carmele, M. Richter, W. W. Chow, and A. Knorr, Inductive equation of motion approach for a semiconductor QD-QED: Coherence induced control of photon statistics, *Phys. Status Solidi (b)* **248**, 872 (2011).
- [28] V. Chernyak and S. Mukamel, Collective coordinates for nuclear spectral densities in energy transfer and femtosecond spectroscopy of molecular aggregates, *J. Chem. Phys.* **105**, 4565 (1996).
- [29] W. M. Zhang, T. Meier, V. Chernyak, and S. Mukamel, Exciton-migration and three-pulse femtosecond optical spectroscopies of photosynthetic antenna complexes, *J. Chem. Phys.* **108**, 7763 (1998).
- [30] G. Panitchayangkoon, D. Hayes, K. A. Fransted, J. R. Caram, E. Harel, J. Wen, R. E. Blankenship, and G. S. Engel, Long-lived quantum coherence in photosynthetic complexes at physiological temperature, *Proc. Natl. Acad. Sci. U.S.A.* **107**, 12766 (2010).
- [31] T. Kramer, M. Noack, J. R. Reimers, A. Reinefeld, M. Rodriguez, and S. Yin, Energy flow in the Photosystem I supercomplex: Comparison of approximative theories with DM-HEOM, *Chem. Phys.* **515**, 262 (2018).
- [32] R. F. Oulton, V. J. Sorger, D. Genov, D. Pile, and X. Zhang, A hybrid plasmonic waveguide for subwavelength confinement and long-range propagation, *Nat. Photonics* **2**, 496 (2008).
- [33] M. I. Stockman, Nanofocusing of Optical Energy in Tapered Plasmonic Waveguides, *Phys. Rev. Lett.* **93**, 137404 (2004).
- [34] A. Orioux, M. A. Versteegh, K. D. Jöns, and S. Ducci, Semiconductor devices for entangled photon pair generation: A review, *Rep. Prog. Phys.* **80**, 076001 (2017).
- [35] M. Weiß and H. J. Krenner, Interfacing quantum emitters with propagating surface acoustic waves, *J. Phys. D* **51**, 373001 (2018).
- [36] H. Jayakumar, A. Predojević, T. Kauten, T. Huber, G. S. Solomon, and G. Weihs, Time-bin entangled photons from a quantum dot, *Nat. Commun.* **5**, 4251 (2014).
- [37] A. Carmele and S. Reitzenstein, Non-Markovian features in semiconductor quantum optics: Quantifying the role of phonons in experiment and theory, *Nanophotonics* **8**, 655 (2019).
- [38] M. Richter and S. Mukamel, Collective two-particle resonances induced by photon entanglement, *Phys. Rev. A* **83**, 063805 (2011).
- [39] M. Gegg, A. Carmele, A. Knorr, and M. Richter, Super-radiant to subradiant phase transition in the open system Dicke model: Dark state cascades, *New J. Phys.* **20**, 013006 (2018).
- [40] S. Arranz Regidor, G. Crowder, H. Carmichael, and S. Hughes, Modeling quantum light-matter interactions in waveguide QED with retardation, nonlinear interactions, and a time-delayed feedback: Matrix product states versus a space-discretized waveguide model, *Phys. Rev. Research* **3**, 023030 (2021).
- [41] Y. Tanimura and R. Kubo, Time evolution of a quantum system in contact with a nearly Gaussian-Markoffian noise bath, *J. Phys. Soc. Jpn.* **58**, 101 (1989).

- [42] F. Caycedo-Soler, A. Mattioni, J. Lim, T. Renger, S. F. Huelga, and M. B. Plenio, Exact simulation of pigment-protein complexes: Vibronic renormalisation of electronic parameters in ultrafast spectroscopy, [arXiv:2106.14286](https://arxiv.org/abs/2106.14286).
- [43] J. Prior, I. de Vega, A. W. Chin, S. F. Huelga, and M. B. Plenio, Quantum dynamics in photonic crystals, *Phys. Rev. A* **87**, 013428 (2013).
- [44] D. Gribben, D. M. Rouse, J. Iles-Smith, A. Strathearn, H. Maguire, P. Kirton, A. Nazir, E. M. Gauger, and B. W. Lovett, Exact dynamics of Non-additive Environments in Non-Markovian Open Quantum Systems, Quantum dynamics in photonic crystals, *Phys. Rev. X Quantum* **3**, 010321 (2022).
- [45] M. Cygorek, M. Cosacchi, A. Vagov, V. M. Axt, B. W. Lovett, J. Keeling, and E. M. Gauger, Simulation of open quantum systems by automated compression of arbitrary environments, *Nat. Phys.* (2022).
- [46] F. Liu, A. J. Brash, J. O'Hara, L. M. P. P. Martins, C. L. Phillips, R. J. Coles, B. Royall, E. Clarke, C. Bentham, N. Prtljaga, I. E. Itskevich, L. R. Wilson, M. S. Skolnick, and A. M. Fox, High Purcell factor generation of indistinguishable on-chip single photons, *Nat. Nanotechnol.* **13**, 835 (2018).
- [47] C. P. Dietrich, A. Fiore, M. G. Thompson, M. Kamp, and S. Höfling, GaAs integrated quantum photonics: Towards compact and multi-functional quantum photonic integrated circuits, *Laser Photonics Rev.* **10**, 870 (2016).
- [48] R. Bose, D. Sridharan, H. Kim, G. S. Solomon, and E. Waks, Low-Photon-Number Optical Switching with a Single Quantum Dot Coupled to a Photonic Crystal Cavity, *Phys. Rev. Lett.* **108**, 227402 (2012).
- [49] K. Kuruma, Y. Ota, M. Kakuda, S. Iwamoto, and Y. Arakawa, Time-resolved vacuum rabi oscillations in a quantum-dot-nanocavity system, *Phys. Rev. B* **97**, 235448 (2018).
- [50] J.-H. Kim, C. J. K. Richardson, R. P. Leavitt, and E. Waks, Two-photon interference from the far-field emission of chip-integrated cavity-coupled emitters, *Nano Lett.* **16**, 7061 (2016).
- [51] Y. Sato, Y. Tanaka, J. Upham, Y. Takahashi, T. Asano, and S. Noda, Strong coupling between distant photonic nanocavities and its dynamic control, *Nat. Photonics* **6**, 56 (2012).
- [52] J. Schall, M. Deconinck, N. Bart, M. Florian, M. Helversen, C. Dangel, R. Schmidt, L. Bremer, F. Bopp, I. Hüllen, C. Gies, D. Reuter, A. D. Wieck, S. Rodt, J. J. Finley, F. Jahnke, A. Ludwig, and S. Reitzenstein, Bright electrically controllable quantum-dot-molecule devices fabricated by *in situ* electron-beam lithography, *Adv. Quantum Technol.* **4**, 2100002 (2021).
- [53] P. M. Vora, A. S. Bracker, S. G. Carter, T. M. Sweeney, M. Kim, C. S. Kim, L. Yang, P. G. Brereton, S. E. Economou, and D. Gammon, Spin-cavity interactions between a quantum dot molecule and a photonic crystal cavity, *Nat. Commun.* **6**, 7665 (2015).
- [54] J.-H. Kim, S. Aghaeimeibodi, C. J. K. Richardson, R. P. Leavitt, and E. Waks, Super-radiant emission from quantum dots in a nanophotonic waveguide, *Nano Lett.* **18**, 4734 (2018).
- [55] M. Khoshnegar, T. Huber, A. Predojević, D. Dalacu, M. Prilmüller, J. Lapointe, X. Wu, P. Tamarat, B. Lounis, P. Poole, G. Weihs, and H. Majedi, A solid state source of photon triplets based on quantum dot molecules, *Nat. Commun.* **8**, 15716 (2017).
- [56] C. Carlson, D. Dalacu, C. Gustin, S. Haffouz, X. Wu, J. Lapointe, R. L. Williams, P. J. Poole, and S. Hughes, Theory and experiments of coherent photon coupling in semiconductor nanowire waveguides with quantum dot molecules, *Phys. Rev. B* **99**, 085311 (2019).
- [57] S. Mukamel, Superoperator representation of nonlinear response: Unifying quantum field and mode coupling theories, *Phys. Rev. E* **68**, 021111 (2003).
- [58] S. Mukamel, *Principles of Nonlinear Optical Spectroscopy*, Oxford series in optical and imaging sciences (Oxford University Press, New York, 1995).
- [59] H. Grabert, P. Schramm, and G.-L. Ingold, Quantum brownian motion: The functional integral approach, *Phys. Rep.* **168**, 115 (1988).
- [60] G. Vidal, Efficient Classical Simulation of Slightly Entangled Quantum Computations, *Phys. Rev. Lett.* **91**, 147902 (2003).
- [61] See Supplemental Material at <http://link.aps.org/supplemental/10.1103/PhysRevLett.128.167403> for (i) decomposition of tensors, (ii) green functions and model for the photonic crystal cavity system [62], (iii) dipole correlation function and localized detection [63,64], (iv) convergence analysis and consequences of approximate unitary.
- [62] S. Hughes, Coupled-Cavity QED Using Planar Photonic Crystals, *Phys. Rev. Lett.* **98**, 083603 (2007).
- [63] M. Richter, Spatially localized spectroscopy for examining the internal structure of coupled nanostructures, *Phys. Status Solidi (b)* **250**, 1760 (2013).
- [64] J. F. Specht and M. Richter, Reconstruction of exciton wave functions of coupled quantum emitters including spin with ultrafast spectroscopy using localized nanooptical fields, *Appl. Phys. B* **122**, 97 (2016).
- [65] E. M. Stoudenmire and S. R. White, Itensor C++ library, <http://itensor.org/>, 2.1.0 and newer.
- [66] M. Richter, K. J. Ahn, A. Knorr, A. Schliwa, D. Bimberg, M. E.-A. Madjet, and T. Renger, Theory of excitation transfer in coupled nanostructures—from quantum dots to light harvesting complexes, *Phys. Status Solidi (b)* **243**, 2302 (2006).
- [67] M. L. Kerfoot, A. O. Govorov, C. Czarnocki, D. Lu, Y. N. Gad, A. S. Bracker, D. Gammon, and M. Scheibner, Optophononics with coupled quantum dots, *Nat. Commun.* **5**, 3299 (2014).
- [68] A. Zimmermann, S. Kuhn, and M. Richter, Poisson green's function method for increased computational efficiency in numerical calculations of coulomb coupling elements, *Phys. Rev. B* **93**, 035308 (2016).
- [69] A. Nazir and D. P. McCutcheon, Modelling exciton-phonon interactions in optically driven quantum dots, *J. Phys. Condens. Matter* **28**, 103002 (2016).
- [70] S. Lüker, K. Gawarecki, D. Reiter, A. Grodecka-Grad, V. M. Axt, P. Machnikowski, and T. Kuhn, Influence of acoustic phonons on the optical control of quantum dots driven by adiabatic rapid passage, *Phys. Rev. B* **85**, 121302(R) (2012).
- [71] T. Renger and R. Marcus, On the relation of protein dynamics and exciton relaxation in pigment-protein complexes: An estimation of the spectral density and a theory for the calculation of optical spectra, *J. Chem. Phys.* **116**, 9997 (2002).

- [72] R.-C. Ge and S. Hughes, Quantum dynamics of two quantum dots coupled through localized plasmons: An intuitive and accurate quantum optics approach using quasinormal modes, *Phys. Rev. B* **92**, 205420 (2015).
- [73] S. Franke, S. Hughes, M. K. Dezfouli, P. T. Kristensen, K. Busch, A. Knorr, and M. Richter, Quantization of Quasinormal Modes for Open Cavities and Plasmonic Cavity Quantum Electrodynamics, *Phys. Rev. Lett.* **122**, 213901 (2019).
- [74] P. Yao and S. Hughes, Macroscopic entanglement and violation of Bell's inequalities between two spatially separated quantum dots in a planar photonic crystal system, *Opt. Express* **17**, 11505 (2009).
- [75] Y. Yu, A. M. Delgoffe, A. Miranda, A. Lyasota, B. Dwir, A. Rudra, and E. Kapon, Remote excitation between quantum emitters mediated by an optical Fano resonance, *Optica* **8**, 1605 (2021).
- [76] H. T. Dung, L. Knöll, and D.-G. Welsch, Three-dimensional quantization of the electromagnetic field in dispersive and absorbing inhomogeneous dielectrics, *Phys. Rev. A* **57**, 3931 (1998).
- [77] The maximum bond dimension of the MPS in all numerical calculations is truncated to below 200 and an accuracy of $\epsilon = 10^{-12}$, ΔT convergence is discussed in [61].
- [78] L. Yang and S. Mukamel, Two-Dimensional Correlation Spectroscopy of Two-Exciton Resonances in Semiconductor Quantum Wells, *Phys. Rev. Lett.* **100**, 057402 (2008).
- [79] J. Kim, S. Mukamel, and G. D. Scholes, Two-dimensional electronic double-quantum coherence spectroscopy, *Acc. Chem. Res.* **42**, 1375 (2009).
- [80] M. Richter, F. Schlosser, M. Schoth, S. Burger, F. Schmidt, A. Knorr, and S. Mukamel, Reconstruction of the wave functions of coupled nanoscopic emitters using a coherent optical technique, *Phys. Rev. B* **86**, 085308 (2012).
- [81] F. Schlosser, A. Knorr, S. Mukamel, and M. Richter, Using localized double-quantum-coherence spectroscopy to reconstruct the two-exciton wave function of coupled quantum emitters, *New J. Phys.* **15**, 025004 (2013).